

# Reparametrizing the loop entropy weights: effect on DNA melting curves

Ralf Blossey and Enrico Carlon

Interdisciplinary Research Institute c/o IEMN, Cité Scientifique BP 69, F-59652 Villeneuve d'Ascq, France

(Dated: October 30, 2018)

Recent advances in the understanding of the melting behavior of double-stranded DNA with statistical mechanics methods lead to improved estimates of the weight factors for the dissociation events of the chains, in particular for interior loop melting. So far, in the modeling of DNA melting, the entropy of denaturated loops has been estimated from the number of configurations of a closed self-avoiding walk. It is well understood now that a loop embedded in a chain is characterized by a loop closure exponent  $c$  which is higher than that of an isolated loop. Here we report an analysis of DNA melting curves for sequences of a broad range of lengths (from 10 to  $10^6$  base pairs) calculated with a program based on the algorithms underlying MELTSIM. Using the embedded loop exponent we find that the cooperativity parameter is one order of magnitude bigger than current estimates. We argue that in the melting region the double helix persistence length is greatly reduced compared to its room temperature value, so that the use of the embedded loop closure exponent for real DNA sequences is justified.

PACS numbers: 87.14.Gg, 87.15.He, 05.70.Fh, 64.10+h

## I. INTRODUCTION

A standard method to unbind the two strands of a double-stranded DNA (dsDNA) in solution is that of increasing the temperature of the system. This process, known as DNA thermal denaturation or DNA melting, has been studied since the sixties as it provides important information about the interaction between base pairs, the stability of the double helix, the effect of the solvent and of the salt concentration (for a review see Ref. [1]).

Several techniques are currently available for the investigation of DNA thermal denaturation such as UV absorption, differential scanning calorimetry, circular dichroism, NMR, fluorescence emission and temperature gradient gel electrophoresis [2]. Perhaps the most established of these is the UV absorption method which consists in irradiating the sample with UV light at 270 nm, a wavelength which is preferentially absorbed by single stranded DNA (ssDNA). The total fraction of absorbed light,  $\tilde{A}$ , is therefore simply proportional to the fraction of dissociated base pairs of the sequence and provides a direct measurement of the order parameter of the problem. In experimental studies, rather than analyzing directly  $\tilde{A}$ , it is customary to consider its temperature derivative: the plot of  $d\tilde{A}/dT$  vs.  $T$  is known as the differential melting curve [1], but we will simply refer to it, in the rest of the paper, as the melting curve.

Melting curves can show a single or several peaks (typical examples, as observed in experiments, are shown in Fig. 1) whose positions and heights depend on the sequence length and composition as well as on external parameters as the salt concentration. For very short sequences, i.e. of about  $10^2 - 10^3$  base pairs (bps), the melting curve shows a single peak indicating a sudden unbinding of the two strands (see Fig. 1(a)). The peak is rounded by finite size effects and thus can become quite broad for very short chains. Somewhat longer sequences ( $\approx 10^3 - 10^4$  bps) are instead characterized by several

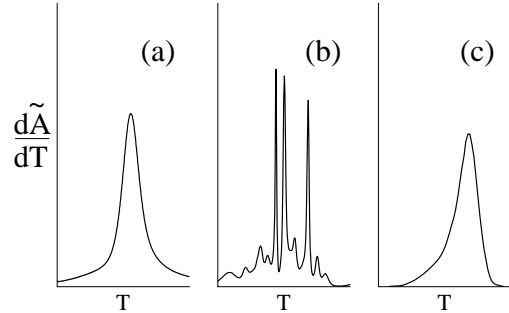


FIG. 1: Schematic view of possible differential melting curves observed for (a) short ( $\approx 10^2$  bps), (b) intermediate ( $\approx 10^3 - 10^4$  bps) and (c) long ( $> 10^6$  bps) DNA sequences.

peaks of typical width of about  $0.5^\circ C$  or less (Fig. 1(b)). These peaks are the signatures of sharp transitions of cooperatively melting regions, as for instance inner loop openings or the unbinding of double stranded regions at the edges of the chain. Finally, in very long chains ( $\approx 10^6$  bps) there is again only a single broad peak covering about  $15 - 20^\circ C$ , which is actually the superposition of many distinct peaks associated with the denaturation of single domains [Fig. 1(c)]. These single peaks cannot be resolved anymore for such long sequences and the melting curve becomes again rather featureless.

The computational prediction of DNA melting curves is a basic bioinformatics task which is needed for a large variety of applications such as primer design, DNA control during Polymerase Chain Reaction or mutation analysis [3]. Also the denaturation behavior of DNA sequences of genomic size is of interest for studies of sequence complexity and evolution and for gene identification and mutation [4, 5, 6, 7]. Consequently, specialized tools, such as Meltsim [8], were developed for this purpose.

The first attempts to model the DNA denaturation

dates back from the sixties (for a recent review see Ref. [9]). The simplest model employed for this purpose was the one-dimensional Ising model where the two spin states  $s_i = 0, 1$  represent the open ( $s_i = 0$ ) or closed ( $s_i = 1$ ) configuration for complementary base pairs [10, 11]. This model obviously does not provide a real thermodynamical phase transition but only a smooth crossover between the closed (dsDNA) and open (ssDNA) regimes. The inclusion of an entropic term, which takes into account the number of possible configurations of the denaturated loops, induces an effective long range interaction in the system and thus a genuine phase transition may occur, as shown long ago by Poland and Sheraga [12].

On rather short DNA sequences ( $\sim 10^2$  bps) the loop entropy contribution is not very important as loops are rare and rather short and the DNA denaturates mainly through unbinding from the edges. A description based on the 1d Ising model with appropriate experimentally determined energy parameters is therefore sufficient (see, e.g., Ref. [13]). A calculation aimed at reproducing experimental melting curves with several peaks of different heights and widths [as that shown in Fig. 1(b)] however needs, besides accurate energy parameters, also a good estimate of the entropy of the denaturated loops.

A broadly known method to calculate DNA melting curves for a given input sequence is the Poland algorithm [14] in which the probability for each base pair to be in an open or closed state can be calculated from a set of recursive relations. The entropy of the denaturated loops is given by counting the number of configurations for a closed self-avoiding walk [15]. This approach overestimates the actual entropy as it does not take into account that the number of configurations available to the loop is limited by the presence of the rest of the chain. Recent advances in the statistical mechanics of polymers provided new insight on how to calculate entropies for loops which are embedded in chains [16, 17].

The aim of this paper is to discuss whether DNA thermal denaturation experiments are able to fix unequivocally the form of the parameters involved in the entropy of denaturated loops. We analyze the effect of the improved loop entropy estimate on the melting curves for DNA sequences of various lengths (up to  $5 \times 10^6$  base pairs) and compositions. We show that the modification of the entropic parameters associated with the loops may have quite a strong effect on the melting curves, especially for sequences of intermediate lengths where several peaks are present [as in the example of Fig. 1(b)]. We also discuss how the effects described here can be best measured experimentally.

This paper is organized as follows: In Sec. II we review some recent results on the entropy of loops embedded into a chain. In Sec. III we present some melting curves for sequences of various lengths and investigate the effect of a modification of the parameters associated with the loop entropy on these curves. In Sec. IV we discuss how the double helix rigidity could influence the results for the

entropy, while Sec. V concludes the paper.

## II. ENTROPY OF A LOOP EMBEDDED IN A CHAIN

In the Poland algorithm the partition function of a loop of total length  $l$  is given by the number of configurations of a self-avoiding walk returning for the first time to the origin [15] after  $l$  steps (Fig. 2(a)), which in the limit  $l \rightarrow \infty$  assumes the following form [18]:

$$L_l \sim \sigma \frac{\mu^l}{l^c} \quad (1)$$

where  $\mu$  is a nonuniversal geometric factor, while  $c$ , the so called loop closure exponent, is a universal quantity. In Eq. (1) we also included a prefactor  $\sigma$ , which only makes sense when comparing the loop partition function with that of a double stranded helix, and measure the absolute probability of interrupting a double helix to open a loop. This quantity is known as the *cooperativity parameter*.

A small value of  $\sigma$  suppresses loop formation so that loops proliferate only at temperatures very close to the melting point and are typically large in order to minimize the effect of a small  $\sigma$ . The transition becomes highly cooperative, in the sense that large portions of the chain will tend to unbind simultaneously. On the contrary, for a  $\sigma \approx 1$ , there is no extra big penalty for loop openings and many small loops may form already well below the melting point. The transition is less cooperative, and peaks in the melting curves appear more rounded-off.

For self-avoiding walks embedded in a three dimensional space the exponent  $c$  has been estimated numerically to be  $c \approx 1.75$  [18]. Other loop parameters have to be fixed by fitting to the available experimental data. In particular, a lot of effort has been devoted to the measurement of the cooperativity parameter  $\sigma$ . Its most accurate determination was performed by Blake and Delcourt [19] who analyzed the melting of several tandemly repeated inserts on a linearized plasmid DNA and found that the value  $\sigma = 1.26 \times 10^{-5}$  fits best the experimental melting curves. This value is consistent with previous estimates [1, 20, 21, 22].

Recent developments in the field of polymer physics allow us to calculate the total number of configurations for a loop embedded in a chain, as for those shown in Fig.

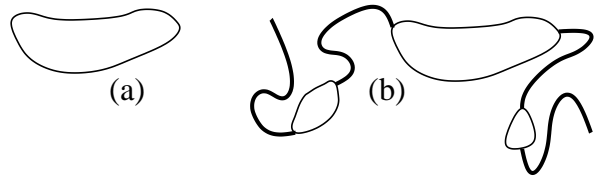


FIG. 2: The total number of configuration for a self-avoiding loop is given by Eq. (1) with  $c \approx 1.75$  for an isolated loop (a) and  $c \approx 2.15$  for a loop embedded in a chain (b).

2(b). Analytical estimates, relying on the general theory of polymer networks [23], indicate that the form given in Eq. (1) is still valid, however with a higher value for the exponent  $c$  [16]. The reason for the higher value of  $c$  is the lower number of configurations available for the loop due to the presence of the rest of the chain, compared to the number of configurations available for an isolated loop. Monte Carlo simulations on suitable three dimensional lattice models yield  $c \approx 2.15$  [17, 24], a value which is also in agreement with analytical estimates, which place this exponent in the range  $2.10 \lesssim c \lesssim 2.20$  [16]. It is also well-known [12, 15] that increasing the value of  $c$  has an effect of sharpening the transition. A value  $c > 2$  implies a first order transition in the case that the energy difference between different base pairs is neglected [12, 15]; first order melting was indeed found numerically [25].

It is clear that accepting  $c = 2.15$  as the most appropriate estimate of the loop exponent entering in the partition function (1) implies that the existing estimate of the cooperativity parameter  $\sigma$  has to be revisited as its experimental determinations relied on the choice  $c = 1.75$ . The aim of this paper is to investigate this issue in detail. To this purpose we analyze the melting curves for DNA sequences of a wide range of lengths up to the full genome of the *E. coli* which amounts to  $5 \times 10^6$  bps.

### III. CALCULATION OF MELTING CURVES

The calculations of DNA melting curves are obtained from our own C-version of the Meltsim package (for details concerning this program, see Ref. [8]), which is a program based on the Poland recursive algorithm for the calculation of the probabilities  $A(i)$  that the  $i$ -th base pair is in a open state. The program uses the Fixman-Friere [26] method, which consists of approximating the loop partition function of Eq. (1) as a sum of  $I$  exponentials:

$$L_l \approx \sigma \sum_{k=1}^I a_k e^{-b_k l} \quad (2)$$

where  $a_k$  and  $b_k$  are fitting coefficients. As for a sequence of total length  $N$  the longest possible loop corresponds to  $l = 2N$ , the fitting is done in a limited interval of lengths. Therefore, the shorter the sequence, the smaller is the number of coefficient  $I$  necessary to obtain a very good fit of Eq. (1) for the relevant loop lengths for the problem. Typically a sum with  $I \approx 10$  coefficients is sufficient for our needs. The advantage of the exponential approximation is that it reduces the computational time for a sequence of  $N$  base pairs from  $O(N^2)$  to  $O(N \times I)$  without any significant loss in accuracy [26].

For various temperatures we calculated  $A(i)$ , the probability that the  $i$ -th base pair is in an open state. From numerical differentiation of the average:

$$A = \frac{1}{N} \sum_{i=1}^N A(i) \quad (3)$$

TABLE I: Domains from pN/MCSx from Ref. [19] considered here as insertions into purely CG-domains.

Seq. (x)	Length (N)	Composition
1	155	[ACTCGGACGA] <sub>15</sub> ACTCG
2	305	[ACTCGGACGA] <sub>30</sub> ACTCG
5	335	[ACTCGGACGA] <sub>33</sub> ACTCG
10	500	[AAGTTGAACAAAT] <sub>38</sub> AAGTTG
11	747	[AAGTTGAACAAAT] <sub>57</sub> AAGTTG
12	214	[AAGTTGAACAAAT] <sub>16</sub> AAGTTG
13	245	[AAGTTGAACAAAAT] <sub>17</sub> AAGTTGA
14	203	[AAGTTGAACAAAAT] <sub>14</sub> AAGTTGA
3	135	[AAGTTGAACAT] <sub>13</sub> AAGTTG
6	330	[AAGTTGAACAAT] <sub>27</sub> AAGTTG
15	292	[AGTGACAT] <sub>36</sub> AGTG

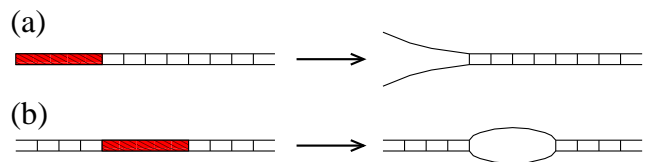


FIG. 3: Schematic view of the melting of the AT-rich insert (gray) in the case of (a) edge insertion and (b) inner insertion as performed in Ref. [19]. The difference in the melting temperatures for the two cases  $\Delta T_M = T_M^{\text{loop}} - T_M^{\text{end}}$  allows to estimate of the cooperativity parameter.

for a sequence of  $N$  base pairs, we obtained the melting curves  $dA/dT$  vs.  $T$ .

In this work we have chosen the ten stacking energy parameters given in Ref. [8]. Another parameter that needs to be specified in the calculation is the concentration of the monovalent salt in solution, which in our calculation varies between 0.05 M and 0.1 M.

#### A. Melting of short sequences

We first analyzed a series of existing experimental data [19] for short sequences consisting of oligomeric repeat patterns shown in Table I. These sequences were inserted in a linearized recombinant pN/MCSx plasmid ( $x$  abbreviates a specific sequence). The insertions are AT-rich and melt at lower temperatures than the rest of the plasmid chain, which plays the role of an energetic barrier to prevent further melting. The insertions were placed at one end, and in the middle of the linearized plasmid, thus their melting occurs through end or loop openings, respectively (see Fig. 3).

The experimental results, tabulated in Ref. [19], are re-analyzed here using the exponent  $c = 2.15$ , appropriate for a loop inserted in a chain. To induce both loop and end openings we embedded the sequences of Table I in the middle and at one end of a pure CGCGCG chain. Due

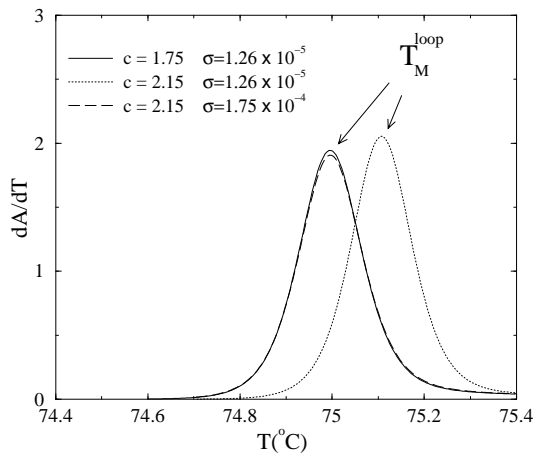


FIG. 4: Calculated melting curves for the Seq. 11 inserted in the middle of a long CGCG... matrix, for 0.075 M of monovalent salt concentration and three choices of  $c$  and  $\sigma$ .

to the higher stability of the CG-domains, their melting will occur at much higher temperatures than those of the inserted sequences.

Figure 4 shows a plot of the differential melting curves for the Seq. 11 of Table I, embedded in the middle of a CG matrix, as calculated by our program. We first fixed  $\sigma = 1.26 \times 10^{-5}$ , the value reported in [19]. The change of  $c$  from 1.75 to 2.15 causes a shift of the position of the melting curves peak of about  $0.2^\circ\text{C}$  and a slight increase of height (the peak position defines the loop melting temperature  $T_M^{\text{loop}}$ ). By choosing  $c = 2.15$ ,  $\sigma = 1.75 \times 10^{-4}$  one recovers a melting curve which almost perfectly overlaps the original one obtained with  $c = 1.75$ ,  $\sigma = 1.25 \times 10^{-5}$  (solid and dashed lines of Fig. 4). This curve fits well the experimental data (see Ref. [19]), thus we conclude that for the choice  $c = 2.15$  and  $\sigma = 1.75 \times 10^{-4}$  yields a melting curve consistent with the experimental values.

In order to provide an estimate of  $\sigma$  from several independent measurements we reanalyzed the procedure followed in Ref. [19]. Figure 5 shows experimental data (empty circles) for the temperature difference of the sequences of Table I,  $\Delta T_M \equiv T_M^{\text{loop}} - T_M^{\text{end}}$ , plotted as functions of the inverse domain length  $1/N$  (data taken from Table I of Ref. [19]). Here  $T_M^{\text{loop}}$  and  $T_M^{\text{end}}$  denote the location of the maxima of  $dA/dT$  for sequences inserted in the interior and at the end of the plasmid chain. The dashed line shows the calculated  $\Delta T_M$  in the case of  $c = 1.75$   $\sigma = 1.26 \times 10^{-5}$ , where the latter value was determined using a regression analysis to fit the experimental data. We have repeated this procedure here fixing  $c = 2.15$  for which we find an equally good fit of the data with the choice  $\sigma = 1.25 \times 10^{-4}$ . Given the precision of the experimental data which we could not assess or analyze further, we find that our calculated curve matches the data very well. Deviations between both theoretical curves clearly appear for shorter chains (loops) where the

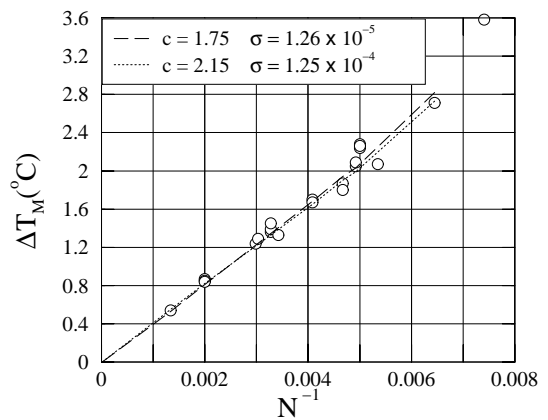


FIG. 5: Plot of  $\Delta T_M$  as function of the inverse domain size. Empty circles are experimental data taken from [19] (Table I) dashed and dotted lines refer to two choices of  $c$  and  $\sigma$ .

application of the asymptotic form of the loop partition function of Eq. (1) may not be appropriate.

## B. Melting of sequences of intermediate length

We next consider the melting of two sequences of intermediate length. We used two protein-coding cancer-related genes, eIF-4G (2900 bps) and LAMC1 (7900 bps), selected from a series of other sequences analyzed for their predominant loop melting effects.

Figure 6(a) shows the melting curves for three different values of  $c$  and  $\sigma$  for a fragment of DNA of eIF-4G as calculated from our program. Four major distinct peaks, labeled from 1 to 4 are visible. The *denaturation maps*, i.e. plots of  $1 - A(i)$  as function of  $i$ , the base position along the chain, which are shown in Fig. 6(b), provide further insight on the type of transitions associated with each peak. We recall that  $1 - A(i)$  is the average probability that the  $i$ -th base pair is in a closed state. The six plots of Fig. 6(b), labeled as  $\alpha, \beta \dots \phi$ , correspond to the six temperatures marked by the vertical arrows in Fig. 6(a).

Comparing the configurations at the temperatures just below and above the peak 3 ( $\gamma$  and  $\delta$ ) we notice that this peak corresponds to the opening of a big loop extending roughly from base pair 1300 to 2300. The melting curves were calculated for three different sets of parameters, starting from the standard choice  $c = 1.75$ , the value associated with isolated loops, together with  $\sigma = 1.26 \times 10^{-5}$ , which is the most recent estimate for the cooperativity parameter [19]. While keeping  $\sigma$  fixed we first consider the exponent for a loop embedded in the chain  $c = 2.15$ . For such a combination of parameters the melting peaks 1 and 2 are shifted from their positions, while peak 4 vanishes in the signal background. The main influence of a change in  $c$  is on peak 3, which for  $c = 2.15$  becomes roughly twice as high ( $dA/dT|_{\text{max}} \approx 1.1$  com-

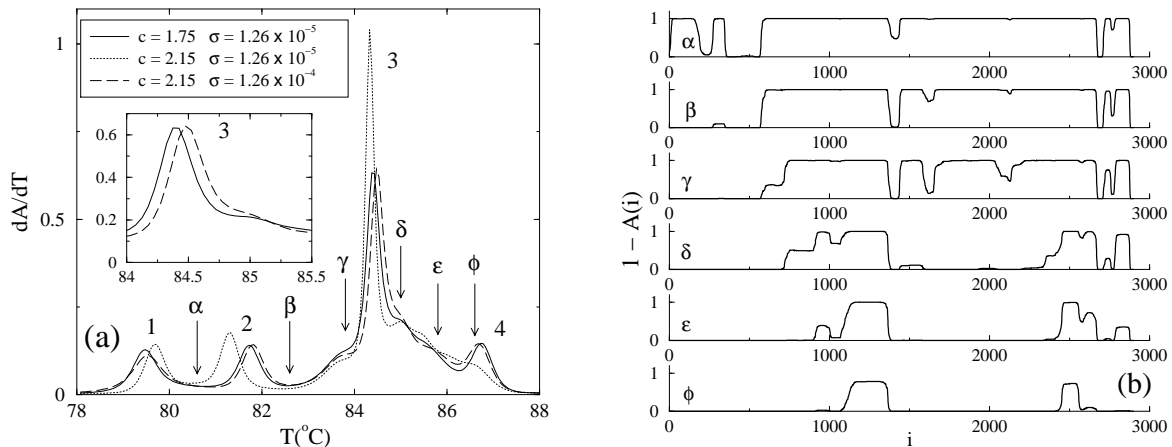


FIG. 6: (a) Melting curves for the sequence eIF-4G for three choices of  $c$  and  $\sigma$  and 0.05 M of monovalent salt. (b) Denaturation maps for  $c = 2.15$ ,  $\sigma = 1.26 \times 10^{-5}$  calculated at the six different temperatures (labeled by  $\alpha, \beta \dots$ ) indicated by vertical arrows in (a).

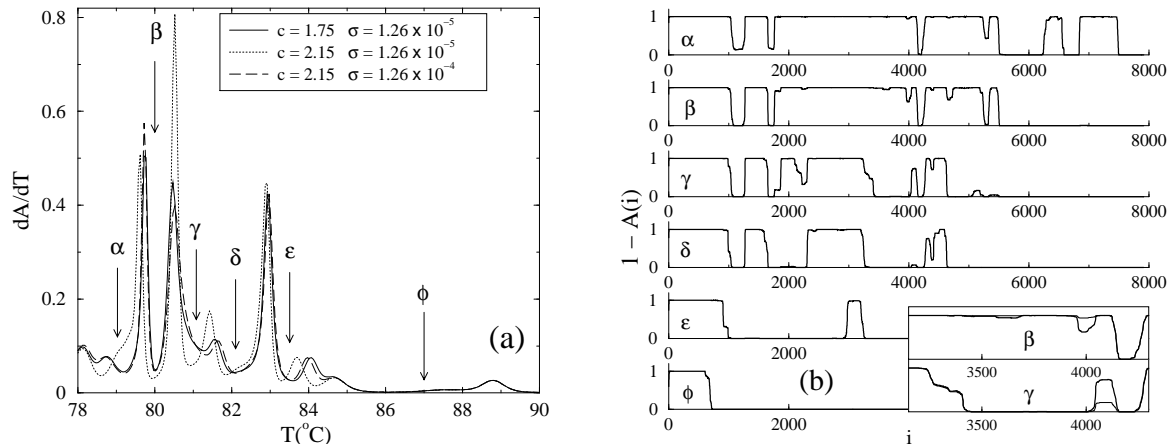


FIG. 7: (a) Plot of the melting curves for the DNA sequence of LAMC1 for three choices of the parameters  $c$  and  $\sigma$ . (b) Denaturation maps for  $c = 2.15$ ,  $\sigma = 1.26 \times 10^{-4}$  at the six different temperatures marked in (a) by the vertical arrows. Inset: Blow up of the denaturation maps  $\beta$  and  $\gamma$  for  $c = 2.15$ ,  $\sigma = 1.26 \times 10^{-4}$  (thick solid lines) and  $c = 2.15$ ,  $\sigma = 1.26 \times 10^{-5}$  (thin solid lines).

pared to  $dA/dT|_{\max} \approx 0.6$  in the case  $c = 1.75$ ). The reason for this is that, as shown from the study of the denaturation maps, the peak 3 corresponds to the opening of a long loop of about 1000 bps, thus any modification of the parameters entering in the loop entropy will have a particularly strong effect on it. Increasing  $c$ , while keeping  $\sigma$  fixed makes the transition sharper, as expected [12, 15].

The third melting curve we plotted is obtained again with  $c = 2.15$ , but with a cooperativity parameter which is one order of magnitude larger:  $\sigma = 1.26 \times 10^{-4}$ . This curve overlaps quite well with the original one. The region where the first and third curves differ the most is around peaks 3 and 4, where the chain contains a 1000 bps long loop, and is shown in the inset of Fig. 6(a). Even in this region the differences are not very big: e.g., the shift of the maximum for peak 3 is  $\Delta T_{\max} \approx 0.1^\circ$ ,

while both peaks keep the same heights.

We repeated similar calculations for other sequences in the same range of lengths. Figure 7(a) shows the melting curves for a fragment of LAMC1 about 7900 bps long, for the same choice of parameters as in Fig. 6. Compared to the previous example there is a larger number of peaks, as the sequence is more than twice as long as the previous one and more subtransitions take place. The most relevant difference between the melting curves calculated for different values of  $c$  and  $\sigma$  is within the region around  $81^\circ\text{C}$ , where a melting peak doubles its height going from the original choice of  $c = 1.75$  to  $c = 2.15$ , while keeping the cooperativity parameter fixed at  $\sigma = 1.26 \times 10^{-5}$ . As in the eIF-4G sequence, when  $\sigma$  is rescaled by a factor 10 we obtain a melting curve running extremely close to the original one in the whole range of temperatures.

It is interesting to take a closer look at the average con-

figurations around the peak at  $T = 80.5^\circ\text{C}$ . The inset of Fig. 7(b) shows a blow up of the denaturation maps  $\beta$  and  $\gamma$  in a region around base pairs  $i = 3500 - 4000$ , where a loop opening occurs. While keeping  $c = 2.15$  we plot in the inset the maps both for  $\sigma = 1.26 \times 10^{-5}$  (thin lines) and  $\sigma = 1.26 \times 10^{-4}$  (thick lines). It is remarkable how little thick and thin lines differ, compared to the big effect of a change of  $\sigma$  in the differential melting curves of Fig. 7(a). The "robustness" of the denaturation maps with respect to a change of the thermodynamic parameters has also been observed recently by Yeremian [4]. The curves in the inset clearly demonstrate the increase of cooperativity when  $\sigma$  is decreased: Either loops are suppressed (case  $\beta$ ) or two neighboring loops tend to merge (case  $\gamma$ ) in order to minimize the effect of a small value of  $\sigma$ . Although the peak at  $83^\circ\text{C}$  corresponds to the formation of a loop of about 2000 bps, as can be seen from the denaturation maps  $\delta$  and  $\varepsilon$ , a change in the loop parameters  $c$  and  $\sigma$  does not seem to modify much this peak, as the transition considered is not an opening of a double helical segment, but rather a merging of two loops with a corresponding enlargement. We conclude that loops merging transitions are less affected by a change in  $c$  and  $\sigma$  as compared to a genuine loop opening.

We notice also that changing the loop parameters do not affect at all the small peak at  $T \approx 89^\circ\text{C}$ , because this corresponds to a transition not involving inner loops, but rather the melting of the region  $0 < i < 900$  through opening from the edges (see  $\phi$  in Fig. 7(b)).

### C. Melting of long sequences (E-Coli)

In order to further assess the validity of the previous analysis we calculated melting curves for much longer DNA sequences ( $\sim 10^6$  bps). Longer sequences have the advantage that they develop loops of a broad range of

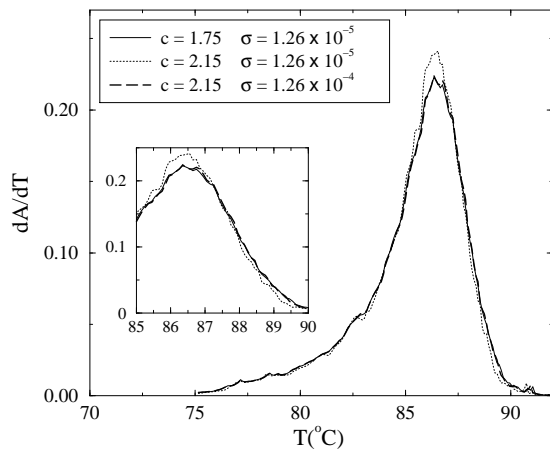


FIG. 8: Melting curves for the whole DNA for E. coli ( $\approx 4,500,000$  bps).

length scales, thus one may test the influence in a change of loop parameters simultaneously for very short and very long loops. Unfortunately a limiting factor in this case is that, as pointed out in the introduction, the melting curves are rather featureless (as for Fig. 1(c)).

Figure 8 show the calculated melting curves for the full DNA of E. coli which is of about  $4.6 \times 10^6$  bps with a known sequence (taken from [27]). The curves are almost continuous, although some irregular structure is still visible, indicating that the discrete sharp peaks of the underlying sequence have not been completely averaged out. The melting curves extend now over about  $15^\circ\text{C}$  and have a typical asymmetric shape, with a gentle growth in the low temperature region, and a steeper descent above  $T_{\text{max}}$ , the temperature for which  $dA/dT$  is maximal.

As before we calculate the melting curves for three different combinations of the parameters  $c$  and  $\sigma$ . Again we find that by changing the loop closure exponent from  $c = 1.75$  to  $c = 2.15$  while rescaling of  $\sigma$  by one order of magnitude brings the curve back to the original one. The two curves obtained in this way are perfectly overlapping. A change of  $c$  only, while leaving  $\sigma = 1.26 \times 10^5$  makes the melting curve somewhat sharper as observed previously for shorter sequences. However the increase of the peak height is limited to about 10%, a rather small effect compared to the doubling of the height found for some peaks of Figs. 6 and 7.

It is interesting to notice that by changing the loop parameters  $c$  and  $\sigma$  the part of the melting curves for  $T \lesssim T_{\text{max}}$  apparently is not modified much as all three curves plotted in Fig. 8 run with good accuracy on top of each other, in this temperature interval. It is only at  $T \approx T_{\text{max}}$  and above that the curves start separating, as shown in the inset. We also point out that the comparison of experimental and calculated melting curves for E. coli of Ref. [8] show some differences in the high temperature region  $T \gtrsim T_{\text{max}}$ . These differences could be due to some non-equilibrium effects, which are known to be more severe for very long sequences [1].

## IV. EFFECT OF THE DOUBLE HELIX STIFFNESS

There has been some discussion recently about the influence of the stiffness of the double helix on the exponent  $c$  [28, 29]. In the very ideal limit of a loop attached to two infinitely rigid rods, the appropriate value of the loop exponent is the same of that of an isolated loop  $c = 1.75$ , as the loop does not interact with the rest of the chain. The dsDNA has a persistence length which is typically much larger than that of the ssDNA ( $\xi_{\text{ds}} \gg \xi_{\text{ss}}$ ), therefore it is legitimate to question the applicability of the polymer network theory [23], from which a higher loop exponent  $c \approx 2.1$  was derived [16], to real DNA sequences.

A different persistence length between dsDNA and ssDNA was incorporated in lattice Monte Carlo simulations

[17]. In these calculations the exponent  $c$ , estimated from an analysis of the distributions of the loop lengths using realistic values for  $\xi_{ds}$  and  $\xi_{ss}$ , was found to be consistent with that of the case in which the difference between persistence lengths is neglected. However these lattice models did not incorporate a cooperativity parameter.

In Ref. [28] it was estimated that sequences up to 5000 bps are still too short to show any interaction effects between a loop with the rest of the chain, so that the appropriate value of the loop exponent should be that of an isolated loop  $c \approx 1.75$ . There is however still disagreement about this conclusion [29].

Here we would like to point out some effects which have been overlooked in the present literature. The main interest in the exponent  $c$  is that of modeling the DNA melting curves and the melting process typically takes place at around  $80^\circ - 90^\circ$  C (see Figs. 6, 7 and 8). Therefore, in order to discuss the applicability of the higher loop exponent  $c \approx 2.1$  to real DNA sequence, it is the difference in persistence length of dsDNA and ssDNA in this range of temperatures which should be investigated. At room temperatures the persistence lengths are  $\xi_{ds}(T = 20^\circ\text{C}) \approx 500$  Å, while  $\xi_{ss}(T = 20^\circ\text{C}) \approx 40$  Å corresponding to roughly 100 bps and 8 bps, respectively [30]. Both conformational fluctuations and electrostatic interactions contribute to the persistence length of dsDNA in solution [31]. In the limit of high salt concentrations electrostatic interactions are totally screened and the persistence length is expected to scale as function of the temperature as in the classical wormlike chain model [32], i.e.  $\xi = \kappa/T$ , with  $\kappa$  temperature independent. This formula implies a reduction of about 20% of the dsDNA persistence length in the melting region compared to the room temperature value. However the assumption that the electrostatic interactions are totally screened may not be fully justified for the range of salt concentrations used here ( $[Na] = 0.1\text{M}$  or lower). Thus the 20% should be rather considered as an upper bound.

A more relevant effect for the reduction of the dsDNA persistence length is the proliferation of small denatured bubbles within a dsDNA segment. Within the model considered here the characteristic lengths close to melting, as the loop and double helix segment lengths, scale as  $1/\sigma$ . As pointed out before, a large cooperativity (small  $\sigma$ ), would imply typically long loops and long double helical segments. However, the conclusion that short (i.e.  $\sim 10$  bps) loops would be totally suppressed due to the small  $\sigma$ , is too simplistic. Several studies showed that the nearest neighbor model largely underestimates the opening probability for small loops (see the discussion in [1] and references therein), so it cannot be a quantitatively reliable tool at too short length scales. Such short loops are present in real DNA samples.

We can demonstrate this effect explicitly by analyzing the experimental melting curves recently obtained [33] in a study of dsDNA bubble dynamics. This study was performed on short sequences (of about 30 bps) containing an internal AT region surrounded on both sides by short

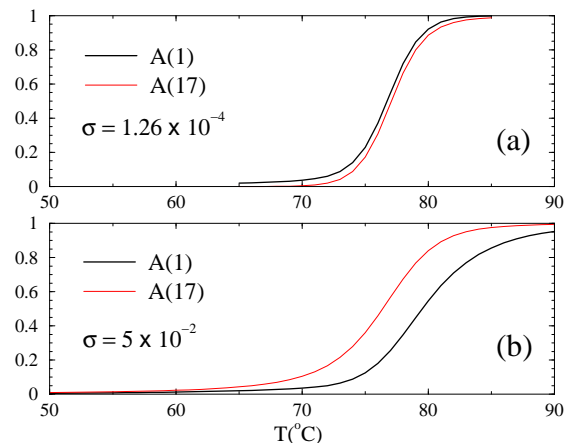


FIG. 9: Probability of finding the  $i = 1$  and  $i = 17$  in an open state plotted as function of the temperature for the sequence  $M_{18}$  of Ref. [33] for  $\sigma = 1.26 \times 10^{-4}$  (a) and  $\sigma = 1.26 \times 10^{-1}$  (b).

CG clamps. Experiments show that the inner AT region melts at temperatures in which the CG edges are still bound [33].

In Fig. 9 we present the calculated melting curves for the probabilities of having the base pair  $i = 1$  and  $i = 17$  in an open state for the sequence  $M_{18}$  of Ref. [33], which can be directly compared with the experimental results as both quantities  $A(1)$  and  $A(17)$  have been measured experimentally through fluorescence measurements [33] (the base pair  $i = 17$  is in the middle of the AT-region). As the sequence is very short the calculated melting curves are not sensitive to a change in  $c$ . For  $\sigma = 1.26 \times 10^{-4}$  (Fig. 9(a)) the typical value for the cooperativity parameter used previously in the paper, our calculations show that  $A(1)$  and  $A(17)$  are at all temperatures very close to each other, which implies that no loops are formed and that the sequence rather melts from edge openings, although the CG edges are energetically more stable than the inner AT region. This is an effect of the small value of  $\sigma$  used in the calculation. In order to verify this we have plotted in Fig. 9(b), just as an illustration, the same quantities with  $\sigma = 5 \times 10^{-2}$ . The reduced cooperativity allows for the formation of loops and now produces results closer to what is observed in experiments (see Fig. 2 of Ref. [33]). Thus, despite that the small cooperativity parameter ( $\sigma \sim 10^{-4}$ ) correctly describes long loop ( $> 100$  bps) formations in DNA melting, small loops ( $\sim 10$  bps) openings in AT-rich domains are still possible. The importance of small bubbles formation in DNA oligomers melting has been recently emphasized in an analysis of the melting of DNA oligomers [34].

As the ssDNA has, at  $90^\circ$  C, an estimated persistence length corresponding to roughly 5 bps, we expect that the opening of a small loop of about 15 bps would be sufficient to decorrelate completely the two dsDNA segments at its two sides. To provide an estimate of the

persistence length of the dsDNA one would need to know the average density of small loops and their probabilities, which depends on the sequence composition. It is however conceivable that this effect would make the dsDNA at 80 – 90°C much more flexible, compared to its room temperature behavior, so that the use of the loop embedded exponent for  $c$  is justified.

## V. CONCLUSION

In this paper we have analyzed the effect of reparametrizing the loop weight contribution, in the calculation of DNA melting curves for sequences of a broad range of lengths, up to the full genome of the E-coli ( $5.6 \times 10^6$  bps). Using the closure exponent for a loop embedded in a chain ( $c = 2.15$ ) we found that in order to reproduce correctly the existing experimental data and melting curves one needs to increase the cooperativity parameter  $\sigma$  by about one order of magnitude. An increase of the cooperativity parameter, which is the weight associated with the interruption of an helix to form a loop, implies that loops are more probable within the chain.

It is clear that a simultaneous change of the loop ex-

ponent  $c$  and of  $\sigma$  cannot reproduce two perfectly overlapping melting curves. We found that rescaling  $\sigma$  by about one order of magnitude together with a change in  $c$  from 1.75 to 2.15 produces typically very small shifts in peak positions ( $\sim 0.1^\circ$ ) and heights. Accurate melting experiments would be able to distinguish between the two choices and fix unequivocally both  $c$  and  $\sigma$ . In any case our analysis indicates that the best samples where to test the above effects are sequences of intermediate lengths ( $\approx 10^3 - 10^4$  bps). We showed that in these sequences rather large loops may be formed and that the associated melting peaks are extremely sensitive to a change in loop parameters  $c$  and  $\sigma$ . The disadvantage of shorter sequences is that they predominantly melt through end openings (unless they are designed to do otherwise, as in the example of the preceding section). The melting curves of very long sequences, as we showed for E. Coli, are only weakly affected by a change in the parameters  $c$  and  $\sigma$ .

**Acknowledgment.** We thank I. Diesinger and E. Meese for their help in finding suitable sequences for melting analysis. Discussions with A. Hanke, R. Metzler and D. Mukamel are gratefully acknowledged.

- 
- [1] R. M. Wartell and A. S. Benight, Phys. Rep. **121**, 67 (1985).
  - [2] V. A. Bloomfield, D. M. Crothers, and I. Tinoco, *Nucleic Acids Structures, Properties and Functions* (University Science Books, Mill Valley, 2000).
  - [3] E. Lyon, Expert Rev. Mol. Diagn. **1**, 92 (2001).
  - [4] E. Yeramian, Gene **255**, 139 (2000).
  - [5] E. Yeramian, Gene **255**, 151 (2000).
  - [6] J. W. Bizzaro, K. H. Marx, and R. D. Blake, in *Materials Science of the Cell*, edited by B. Mulder, V. Vogel and C. Schmidt, MRSC Symposia Proceedings No.489 (Materials Research Society, Pittsburgh, 1998), p.73.
  - [7] T. Garel and H. Orland, eprint cond-mat/0304080.
  - [8] R. D. Blake *et al.*, Bioinformatics **15**, 370 (1999).
  - [9] N. Theodorakopoulos, in *Localization and energy transfer in nonlinear systems* Proceedings of the Third Conference, edited by L. Vázquez, R. S. MacKay, and M. P. Zorzano (World Scientific, Singapore, 2003).
  - [10] B. H. Zimm and J. R. Bragg, J. Chem. Phys. **31**, 526 (1959).
  - [11] B. H. Zimm, J. Chem. Phys. **33**, 1349 (1960).
  - [12] D. Poland and H. A. Scheraga, J. Chem. Phys. **45**, 1456 (1966).
  - [13] R. Owczarzy *et al.*, Biopolymers **44**, 217 (1997).
  - [14] D. Poland, Biopolymers **13**, 1859 (1974).
  - [15] M. E. Fisher, J. Chem. Phys. **44**, 616 (1966).
  - [16] Y. Kafri, D. Mukamel, and L. Peliti, Phys. Rev. Lett. **85**, 4988 (2000).
  - [17] E. Carlon, E. Orlandini, and A. L. Stella, Phys. Rev. Lett. **88**, 198101 (2002).
  - [18] C. Vanderzande, *Lattice models of Polymers* (Cambridge University Press, 1998).
  - [19] R. D. Blake and S. G. Delcourt, Nucleic Acids Res. **26**, 3323 (1998).
  - [20] A. L. Oliver, R. M. Wartell, and R. L. Ratliff, Biopolymers **16**, 1115 (1977).
  - [21] B. R. Amirikyan, A. V. Vologodskii, and Y. L. Lyubchenko, Nucleic Acids Res. **9**, 5469 (1981).
  - [22] R. D. Blake, Biopolymers **26**, 1063 (1987).
  - [23] B. Duplantier, Phys. Rev. Lett. **57**, 941 (1986).
  - [24] M. Baiesi, E. Carlon, and A. L. Stella, Phys. Rev. E **66**, 021804 (2002).
  - [25] M. S. Causo, B. Coluzzi, and P. Grassberger, Phys. Rev. E **62**, 3958 (2000).
  - [26] M. Fixman and J. J. Freire, Biopolymers **16**, 2693 (1977).
  - [27] <http://www.genome.wisc.edu/sequencing/k12.htm>.
  - [28] A. Hanke and R. Metzler, Phys. Rev. Lett. **90**, 159801 (2003).
  - [29] Y. Kafri, D. Mukamel, and L. Peliti, Phys. Rev. Lett. **90**, 159802 (2003).
  - [30] J. F. Marko and E. D. Siggia, Macromolecules **28**, 8759 (1995).
  - [31] T. Odijk, J. Polym. Sci. **15**, 477 (1977); J. Skolnick and M. Fixman, Macromolecules **10**, 944 (1977).
  - [32] M. Doi and S. F. Edwards, *The Theory of Polymer Dynamics* (Oxford University Press, New York, 1989).
  - [33] G. Altan-Bonnet, A. Libchaber, and O. Krichevsky, Phys. Rev. Lett. **90**, 138101 (2003).
  - [34] G. Zocchi, A. Omerzu, T. Kuriabova, J. Rudnick, and G. Grüner, eprint cond-mat/0304567.